International Journal of Fluid Mechanics Research, 44(5):375–385 (2017)

AN ESTIMATION OF TURBULENT SECONDARY FLOW RESISTANCE IN RECTANGULAR DUCTS FROM A FLOW MODEL

Sujit K. Bose

S.N. Bose National Center for Basic Sciences, Salt Lake City, Kolkata 700098, India, E-mail: sujitkbose@yahoo.com

Original Manuscript Submitted: 10/28/2016; Final Draft Received: 2/20/2017

Incompressible fluid flow in smooth rectangular ducts at working streamwise velocities is turbulent because of resistance of the four side-walls. A second feature of such flows is generation of secondary currents, though weak, in transverse cross sections. These secondary currents cause additional flow resistance, resulting in pressure drop in the direction of the primary flow. A number of experimental studies have been reported on the turbulence structure and consequent geometrical structures of the flow. In particular, the two diagonals and the pair of bisectors of the side walls divide a cross section into eight cells, in each of which vortical patches of motion take place. In this paper, it is shown that the vortical motion in a cell is kinematically analogous to the torsion problem of a prismatic isotropic elastic beam. Based on experimental results, the patch vortex in a cell is modeled to have elliptic shape with the major axis thrust toward a corner of the duct, giving a mathematical model of the flow field. Using the expressions for the transverse velocity components in the total momentum equation, with $1/p$*th power law where* $p \approx 7$ *for the streamwise velocity, an equation is obtained between the side-wall resistance due to the secondary flow and the vorticity in each cell of division of the duct. Two particular cases are considered in numerical detail when the duct is square and when the height of the duct is one-half of the base length. For experimental validation of the side-wall resiatance formulae, additional experimental research is needed.*

KEY WORDS: *secondary turbulent flow, rectangular duct, vortex patch, torsion problem of prismatic isotropic beams, side-wall shear resistance*

1. INTRODUCTION

Incompressible turbulent flows in straight rectangular ducts/channels are of importance in many engineering practices, such as in air-conditioning systems and other types of heat exchangers, rotating machineries, and in nuclear-reactor channels. Fully developed turbulent flows are often in these cases due to wall resistance, which is generally three dimensional in nature. The four corners of the duct being farthest from the central axis of the duct compared to the distances from the opposite pair of walls, there is greater flux in the corner directions compared to that in the directions of the side bisectors of the walls of the duct. Kinematically due to such velocity differential, secondary flow is generated in transverse sections of the duct. This phenomenon was first observed by Nikuradze (1926), who noted that the axial isovels bulged outward toward the corners of the duct. In his book, Prandtl (1952), gives a classification that the mean streamwise vorticity in the helical turbulent flow arises not only from the mean flow skewness, but also from the inhomogeneity of the anisotropic wall turbulence. Quantification of the secondary flow was first reported by Hoagland (1960) by hot-wire anemometer technique. This technique was further improved in accuracy by Brundrett and Baines (1964), Gessner (1973), Gessner and Jones (1965), and Launder and Ying (1972). Further improvement in experimental data was achieved by Melling and Whitelaw (1976) by the use of laser Doppler anemometer. It is concluded from the experimental studies that the secondary flow is weak, being about 1% of the streamwise velocity, but causing strong influence on the overall as well as local properties of flow. Other quantities of interest, such as measurement of mean velocity profiles, pressure drop in the streamwise direction, and peripheral wall shear

1064–2277/17/$35.00

stress distribution have been given by Leutheusser (1963) and Ahmed and Brundrett (1971). A complete description of turbulent flow in square ducts was provided by Brundrett and Baines (1964), measuring all six components of Reynolds stress as well as the three components of the mean velocity. Their finding is that kinetically, the secondary current is caused by Reynolds shear stress in planes parallel to the duct cross sections, where the indications are that the shear stresses are caused by gradient of normal stresses. From examination of the result of turbulence production, they also conclude that the axial vorticity cannot exist in laminar flows. Perkins (1970) gives a theory for the direction of the secondary currents based on a simple model of anisotropic turbulence at a corner boundary layer. Gessner (1973), deals with developing turbulent flow along a corner. He shows that a transverse flow is initiated and directed toward a corner as a result of turbulent shear stress gradient normal to the bisector and that the anisotropy of turbulent normal stress does not play a major role in the generation of secondary flow. The accurate measurements of Melling and Whitelaw (1976) quantitatively justify the earlier findings after obtaining plots from experimental measurements for contours of streamwise velocity and turbulence intensity in developing flows and all the three mean velocity components and five of the six Reynolds stresses in nearly fully developed flow.

In this paper, a uniformly steady fully developed turbulent flow is considered in a straight rectangular horizontal duct. Assuming the flow to be ideally symmetric about the two diagonals and the two central bisector axes, it is argued that the secondary flow is vortical in each of the eight cells into which a cross section can be divided by the four axes of symmetry. This circulatory cellular subdivision is supported by experimental findings of Melling and Whitelaw (1976). For the weak secondary circulatory flows, the Reynolds averaged Navier–Stokes (RANS) equations reduce to the continuity equation for the axial vorticity and an axial streamwise momentum equation involving the gradient of components of the Reynolds stress. The experimentally observed circulatory motion in a cell is modeled by an elliptic patch vortex. For this model, the total momentum equation in the streamwise direction yields a formula for the shear resistance exerted on the walls of the duct, in terms of the axial cellular vorticity. Two particular cases are numerically considered to derive explicit formulae for the flow resistance: in a square duct and that in a rectangular duct, one pair of whose parallel sides is one-half of the other pair.

2. GOVERNING EQUATIONS OF THE FLOW

Let the width and height of the duct be 2 and $2h$, respectively, so that the length scale is chosen to be nondimensional at the outset, as schematically shown in Fig. 1. Taking the X axis along the axis of the duct in the direction of the flow, the Y axis parallel to the base, and the Z axis in the vertical direction, the velocity at any point $P(x, y, z)$ has components (u, v, w) that can be split into time-averaged components $(\bar{u}, \bar{v}, \bar{w})$ and fluctuations (u', v', w') due to turbulence generated by the four sides of the duct. Thus,

$$u = \bar{u} + u', \quad v = \bar{v} + v', \quad w = \bar{w} + w' \tag{1}$$

These components satisfy the continuity equation

$$\frac{\partial \bar{u}}{\partial x} + \frac{\partial \bar{v}}{\partial y} + \frac{\partial \bar{w}}{\partial z} = 0 \tag{2}$$

and the forward streamwise momentum equation

$$\frac{\partial \bar{u}}{\partial t} + \bar{u}\,\frac{\partial \bar{u}}{\partial x} + \bar{v}\,\frac{\partial \bar{u}}{\partial y} + \bar{w}\,\frac{\partial \bar{u}}{\partial z} = -\frac{1}{\rho}\,\frac{\partial \bar{p}}{\partial x} + \nu\nabla^2\bar{u} - \frac{1}{\rho}\,\frac{\partial(\overline{u'^2})}{\partial x} + \frac{1}{\rho}\,\frac{\partial \tau_{xy}}{\partial y} + \frac{1}{\rho}\,\frac{\partial \tau_{xz}}{\partial z} \tag{3}$$

The momentum equations in the y and z directions are of second-order smallness in a transverse plane and are are therefore not required. In Eq. (3), $\bar{p}$ = pressure, ν = kinematic coefficient of viscosity, $\tau_{xy} = -\overline{u'v'}$, $\tau_{xz} = -\overline{u'w'}$ are the components of Reynolds shear stress. Since it is assumed that the flow is steady state and uniform in the x direction, $\partial(\cdot)/\partial t = \partial(\cdot)/\partial x = 0$. Moreover, since the motion is assumed to be fully turbulent, the viscous term becomes negligible and so Eqs. (2) and (3) reduce to

$$\frac{\partial \bar{v}}{\partial y} + \frac{\partial \bar{w}}{\partial z} = 0 \tag{4}$$

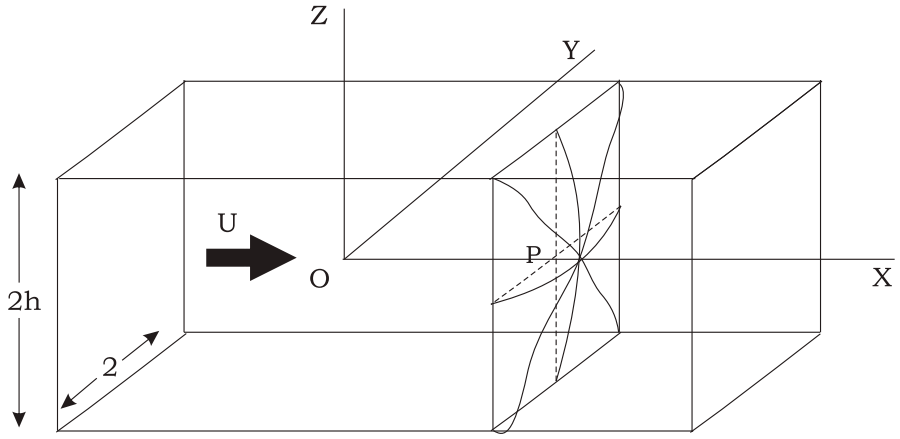

FIG. 1: Forward flow with mean velocity U and surface profile of the streamwise velocity $\bar{u}(x; y; z)$

and

$$\bar{v}\,\frac{\partial \bar{u}}{\partial y} + \bar{w}\,\frac{\partial \bar{u}}{\partial z} = \frac{1}{\rho}\,\frac{\partial \tau_{xy}}{\partial y} + \frac{1}{\rho}\,\frac{\partial \tau_{xz}}{\partial z} \tag{5}$$

Equations (4) and (5) are the only two equations that govern the five unknown quantities: $\bar{u}$, $\bar{v}$, $\bar{w}$, τ_{xy}, and τ_{xz}. Hence, suitable flow modeling is required using available analogies.

3. FLOW MODEL

The profile of the streamwise velocity $\bar{u}$ at a point (x, y, z) is shown in Fig. 1. It is predominantly controlled by "law of the wall" applied to the sides of the duct. This law may be conveniently assumed to be given by the power law with some exponent $1/p$. The value of p is assumed to be equal to 7 as in the case of an infinite plane (Schlichting, 1979, p. 590). Noted that near the four corners of a section, the velocity is of slightly greater magnitude, as stated in the Introduction. This increased value is however ignored for difficulty in modeling the exact profile of $\bar{u}$. Neglecting the very small discrepency on this acoount, $\bar{u}$ is modeled here in the form

$$\bar{u} = U_0\,(1 - y^2)^{1/p}\left[1 - \left(\frac{z}{h}\right)^2\right]^{1/p} \tag{6}$$

where U_0 = constant. If U is the mean velocity of flow as depicted in Fig. 1, then following Eq. (6)

$$U = \frac{U_0}{h}\int_0^1\int_0^h (1 - y^2)^{1/p)}\left[1 - \left(\frac{z}{h}\right)^2\right]^{1/p} dy\,dz = U_0\left[\int_0^{\pi/2} \cos^{(2/p+1)}\theta\,d\theta\right]^2 = U_0\,2^{4/p}\,\frac{[\Gamma(1/p+1)]^4}{[\Gamma(2/p+2)]^2} \tag{7}$$

(Gradshteyn and Ryzhik, 1980, p. 369). For $= 7,\ \Gamma(1/7 + 1)$ and $\Gamma(2/7 + 1)$ are evaluated as 0.93542 and 0.89972, respectively, using an approximation formula for $\Gamma(x + 1),\ (0 \le x \le 1)$ (Abramowitz and Stegun, 1972, p. 257). Equation (7) for $p = 7$ then becomes

$$U = 0.85023\,U_0 \tag{8}$$

The primary streamwise flow profile of $\bar{u}$ given by Eq. (6) in a cross section of the duct is symmetric with respect to y and z. The secondary flow is represented by $\bar{v}$ and $\bar{w}$, governed by Eq. (4). The streamlines of this flow are therefore determined by the stream function $\psi(y,\ z)$ that satisfies Eq. (4) such that

$$\bar{v} = \frac{\partial \psi}{\partial z}, \quad \bar{w} = -\frac{\partial \psi}{\partial y} \tag{9}$$

The secondary flow is circulatory, because the domain is closed. It is determined by a vorticity vector parallel to the streamwise x axis. If ω is the algebraic value of the vorticity measured in the *clockwise sense*, then using Eq. (4)

$$-\omega = \frac{1}{2}\left(\frac{\partial \bar{w}}{\partial y} - \frac{\partial \bar{v}}{\partial z}\right) = -\frac{1}{2}\nabla^2\psi$$

or,

$$\nabla^2\psi = 2\,\omega \tag{10}$$

The rectangular boundary being a streamline, ψ = constant along the boundary. For the weak secondary flow, if it is assumed that the vorticity ω is nearly uniform over a cross section of the duct, then Eq. (10) and the boundary condition show that $\psi/(-\omega)$ is analogous to the Prandl's stress function for the solution of the torsion of an isotropic elastic prismatic beam (Sokolnikoff, 1956, p. 116). The solution for a rectangular beam shows that the solution is not only symmetric about the axes of y and z but also about the diagonals of the beam (Sokolnikoff, 1956, p. 133). This type of symmetry is also roughly observed in the case of rectangular duct flow (Melling and Whitelaw, 1976, Fig. 13). A schematic of the flow is shown in Fig. 2. In the figure, the flow along the two axes converges toward the center, while the flow along the bisecting diagonals diverges toward the four corners. The circulatory flow in each of the octants, starting from the first, are thus assumed to be alternately clockwise and anti-clockwise. A small portion of the latter flow near the corners is drawn in to the main axial flow parallel to the x axis, resulting in some augmentation in the value of $\bar{u}$. Similarly the converging flow toward the center also augments the streamwise flow but the proportion is insignificant as the magnitude of the streamwise flow is comparatively much larger.

4. MATHEMATICAL MODELING OF THE SECONDARY FLOW

From the scheme of the model described in the preceding section, it is clear that it is necessary to consider only one octant of the eight triangular divisions of the rectangle. The mathematical models for the remaining triangular regions are obtainable by simple coordinate transformation. In the following the lower right-angled triangle bounded by the lines $y = 0$, $z = -h$, and $z = -hy$ is considered for qualitative comparison with the experimental observations of Melling and Whitelaw (1976). Assuming ω to be constant in this domain, let

$$\Psi = \psi - \frac{1}{2}(y^2 + z^2), \quad hy + z < 0, \;\; 0 < y < 1, \;\; -h < z < 0 \tag{11}$$

then for Eq. (10),

$$\nabla^2\Psi = 0 \tag{12}$$

in the triangular domain. The boundary C of the region is a streamline along which the stream function ψ = constant = 0, (say), then from Eq. (11)

$$\Psi = -\frac{\omega}{2}(y^2 + z^2), \quad \text{on} \quad C \tag{13}$$

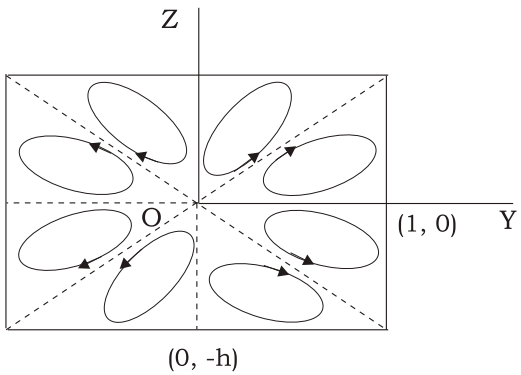

FIG. 2: Schematic of the secondary flow

In the domain under consideration, the vortex motion is clockwise and therefore the vorticity ω must be positive according to the definition adopted earlier. For the motion in the adjascent triangle of the fourth quadrant, ω is to be changed to $-\omega$ due to antisymmetry of the motion, similarly in the remaining cells of the duct.

The function $\Psi/(-\omega)$ solves the the torsion problem of a right angled triangular prismatic beam. An exact solution of the problem when the triangle is isosceles ($h = 1$ case), was given by Galerkin (Sokolnikoff, 1956, p. 134). The solution for the triangular domain under consideration thus takes the form

$$\frac{\Psi}{\omega} = yz' - \frac{1}{2}(y + z') + 4\sum_{n=0}^{\infty} \frac{\sinh k_n((1/2) - z')\, \sin k_n y + \sinh k_n((1/2) - y)\, \sin k_n z'}{k_n^3\, \sinh(k_n/2)} \tag{14}$$

where $z' = z + 1,\ (0 < z' < 1)$ is written for brevity, and $k_n = (2n + 1)\,\pi$. Restoring the variable z, the velocity components of the circulating flow given by Eq. (9), using Eq. (11), become

$$\frac{\bar{v}}{\omega} = \frac{1}{2} + y + z - 4\sum_{n=0}^{\infty} \frac{\cosh k_n((1/2) + z)\, \sin k_n y - \sinh k_n((1/2) - y)\, \cos k_n(z + 1)}{k_n^2\, \sinh(k_n/2)} \tag{15}$$

$$\frac{\bar{w}}{\omega} = -\frac{1}{2} - y - z + 4\sum_{n=0}^{\infty} \frac{\sinh k_n((1/2) + z)\, \cos k_n y + \cosh k_n((1/2) - y)\, \sin k_n(z + 1)}{k_n^2\, \sinh(k_n/2)} \tag{16}$$

The velocity field given by Eqs. (15) and (16) is plotted in Fig. 3. The center of circulation is found to be at the centroid of the triangular section. This type of flow model follows the observation of Brundrett and Baines (1964).

Figure 13 of the experimental observation of the secondary flow by Melling and Whitelaw [11], shows distinct difference from the one shown in Fig. 3. The experimental data show oval type of swirling motion, pushed towards a corner of the duct by the primary streamwise flow along the axis of x. If the oval-shaped vortex patch is modeled by an ellipse of maximum area, with its center on the bisector from the duct corner, then for constant ω in the region, the problem is analogous to the torsion of an isotropic elastic elliptic cylinder (Sokolnikoff, 1956, p. 121). To develop the model, let $O'Y'$, $O'Z'$ be chosen as shown in Fig. 4, so that $y' = y$ and $z' = z + 1$ as before. Also, if the major and minor axes are chosen as axes CX_1 and CZ_1, respectively, then

$$y_1 = (y' - y'_0)\, \cos\alpha - (z' - z'_0)\, \sin\alpha \tag{17a}$$

$$z_1 = (y' - y'_0)\, \sin\alpha - (z' - z'_0)\, \cos\alpha \tag{17b}$$

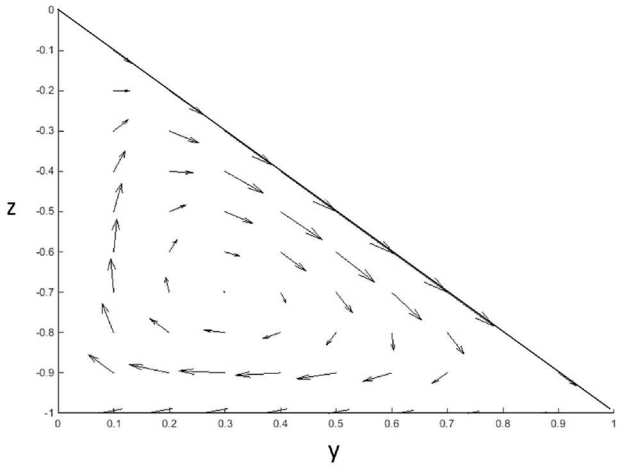

FIG. 3: Velocity field for uniform vorticity ω

where (y_0', z_0') are the coordinates of the center C of the ellipse. If r is the distance of C from the corner $(1,\ 0)$ and 2α is the angle made by the diagonal of the rectangle with the base, then

$$y_0' = 1 - r\ \cos\alpha, \quad z_0' = r\ \sin\alpha \tag{18}$$

It follows that

$$r = \sqrt{(1 - y_0')^2 + z_0'^2} \tag{19}$$

Let the semi-major and minor axes of the ellipse be a and b, then its equation with CX_1 and CY_1 as axes is

$$\frac{y_1^2}{a^2} + \frac{z_1^2}{b^2} = 1 \tag{20}$$

For maximum size of the ellipse, the diagonal $y_1/r + z_1/(r\ \tan\alpha) = 1$ and the base of the triangle $z' = z_0'$, or using Eqs. (17a) and (17b), $-y_1 \sin\alpha + z_1\ \cos\alpha = z_0'$ must touch the ellipse. The condition of tangency for both of the straight lines reduces to the condition

$$b^2 = \tan^2\alpha\,(r^2 - a^2) \tag{21}$$

Assuming that the position of C: $(y_0',\ z_0')$ is known from experimental data subject to the condition that $z_0' = (1 - y_0')\ \tan\alpha$, the area of the ellipse $S = \pi\, ab = \pi\ \tan\alpha\, a\sqrt{r^2 - a^2}$ is maximum when $a = r/\sqrt{2}$, which is permissible if $y_0' > a\ \cos\alpha$ or from Eq. (18), $a < \sec\alpha\,(1 - r\ \cos\alpha) = \sec\alpha - r$. Hence,

$$a = \min\left\{\frac{r}{\sqrt{2}},\ \sec\alpha - r\right\} \tag{22}$$

Equation (21) then determines the value of b.

The equation of the ellipse (20) in parametric form becomes

$$y' = y_0' + a\ \cos\alpha\ \cos\phi + \sqrt{r^2 - a^2}\ \sin\alpha\ \tan\alpha\ \sin\phi \tag{23a}$$

$$z' = z_0' + \sin\alpha\,(\sqrt{r^2 - a^2}\ \sin\phi - a\ \cos\phi) \tag{23b}$$

where $0 \le \phi \le 2\pi$. This form is convenient for computing the ellipse.

Referring to CY_1, CZ_1 as axes of coordinates, the velocity components are $\bar{v}_1 = \partial\psi/\partial z,\ \bar{w}_1 = -\partial\psi/\partial y_1$ as in Eq. (9), where $\partial^2\psi/\partial y_1^2 + \partial^2\psi/\partial z_1^2 = 2\,\omega$ within the ellipse (20) such that $\psi = 0$ on the boundary. Setting $\Psi = \psi - (\omega/2)\,(y_1^2 + z_1^2),\ \nabla^2\Psi = 0$ such that $\Psi/(-\omega) = (1/2)\,(y_1^2 + z_1^2)$. The solution of this problem is thus identical to the solution of the torsion of an isotropic elliptic cylinder (Sokolnikoff, 1956, p. 121), which is given by

$$\frac{\Psi}{-\omega} = \frac{1}{2}\,\frac{a^2 - b^2}{a^2 + b^2}\,(y_1^2 - z_1^2) + \frac{a^2 b^2}{a^2 + b^2} \tag{24}$$

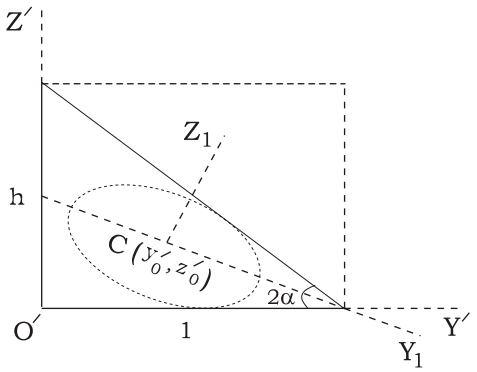

FIG. 4: Elliptic vortex model

where a, b are given by Eqs. (22) and (21). Thus,

$$\bar{v}_1 = \frac{2\omega a^2}{a^2+b^2}\, z_1, \quad \bar{w} = -\frac{2\omega b^2}{a^2+b^2}\, y_1 \tag{25}$$

Hence, by transformation to the $O'Y',\ O'Z'$ system, and using the transformations (17a) and (17b)

$$\begin{aligned}\bar{v} &= \bar{v}_1\,\cos\alpha + \bar{w}_1\,\sin\alpha = \frac{2\omega}{a^2+b^2}\,(a^2\cos\alpha\, z_1 - b^2\sin\alpha\, y_1)\\ &= \frac{2\omega}{a^2+b^2}\left[(a^2-b^2)\,\sin\alpha\,\cos\alpha\,(y'-y'_0) + (a^2\,\cos^2\alpha + b^2\,\sin^2\alpha)\,(z'-z'_0)\right]\end{aligned} \tag{26a}$$

$$\begin{aligned}\bar{w} &= -\bar{v}_1\,\sin\alpha + \bar{w}_1\,\cos\alpha = -\frac{2\omega}{a^2+b^2}\,(a^2\sin\alpha\, z_1 + b^2\cos\alpha\, y_1)\\ &= -\frac{2\omega}{a^2+b^2}\left[(a^2\,\sin^2\alpha + b^2\,\cos^2\alpha)\,(y'-y'_0) + (a^2-b^2)\,\sin\alpha\,\cos\alpha\,(z'-z'_0)\right]\end{aligned} \tag{26b}$$

Equations (26a) and (26b) give the secondary flow velocities due to the elliptic patch vortex. The expressions for $\bar{v}$ and $\bar{w}$ in the original $OXYZ$ system of coordinates are obtained by replacing $y'-y'_0$ and $z'-z'_0$ in Eqs. (26a) and (26b) by $y-y_0$ and $z-z_0$, respectively. Due to maximum size of the ellipse, the velocities outside the patch close to the triangular boundary enclosing the ellipse are satisfied only approximately.

5. THE AVERAGED FORWARD MOMENTUM EQUATION

The forward momentum equation (5) has two unknown Reynolds shear stresses τ_{xy} and τ_{xz}. For drawing conclusion from this single equation, it is averaged over a cross section, which gives

$$\int_{y=0}^{1}\int_{z=-h}^{-hy}\left(\bar{v}\frac{\partial\bar{u}}{\partial y} + \bar{w}\frac{\partial\bar{u}}{\partial z}\right)dz\,dy = \frac{1}{\rho}\int_{z=-h}^{0}\tau_{xy}\Big|_{y=0}^{-z/h}dz + \frac{1}{\rho}\int_{y=0}^{1}\tau_{xz}\Big|_{z=-h}^{-hy}dy = \frac{\tau_0}{\rho} \tag{27}$$

where the shear stress across the two fluid surfaces $y=0$ and $z=-hy$ vanishes because there is no interfacial resistance from the adjacent zones (Fig. 2). The duct surface $z=-h$ induces a shear resistance $\tau_0 = -\tau_{xz}|_{z=-h}$ per unit area on the forward fluid flow, opposite to the axis of x. This results in the first term on the right-hand side of Eq. (27). Using the expressions for $\bar{u}$, $\bar{v}$, and $\bar{w}$ from Eqs. (6), (26a), and (26b), Eq. (27) yields for τ_0 the expression

$$\begin{aligned}\frac{\tau_0}{\rho} = -\frac{4U_0\omega h}{p(a^2+b^2)}\int_{y=0}^{1}\int_{\zeta=-1}^{-y}\Big[&\Big\{(a^2-b^2)\,\sin\alpha\,\cos\alpha\,(y-y_0) + h(a^2\,\cos^2\alpha + b^2\sin^2\alpha)(\zeta-\zeta_0)\Big\}\\ &\times y(1-y^2)^{1/p-1}(1-\zeta^2)^{1/p} - \frac{1}{h}\Big\{(a^2\,\sin^2\alpha + b^2\,\cos^2\alpha)(y-y_0) + h\,(a^2-b^2)\,\sin\alpha\,\cos\alpha\,(\zeta-\zeta_0)\Big\}\\ &\times (1-y^2)^{1/p}\zeta(1-\zeta^2)^{1/p-1}\Big]\,d\zeta\,dy\end{aligned} \tag{28}$$

The double integral in Eq. (28), consists of two parts written within two pairs of braces. The two parts are singular for $y=1$ and $\zeta=-1$, respectively. The singularities of the two terms are removed by setting $y=1-\eta^p$ and $\zeta=\zeta_1^p-1$. By these substitutions and again replacing η by y and ζ_1 by ζ, the equation can be written in the form

$$\begin{aligned}\frac{\tau_0}{\rho} = -\frac{4U_0\omega h}{a^2+b^2}\int_{y=0}^{1}\Big[&\Big\{(A_1(1-y^p)+C_1)\int_{\zeta=-1}^{-(1-y^p)}(1-\zeta^2)^{1/p}\,d\zeta + B_1\int_{\zeta=-1}^{-(1-y^p)}\zeta(1-\zeta^2)^{1/p}\,d\zeta\Big\}\\ &\times(1-y^p)(2-y^p)^{1/p-1} - \frac{1}{h}\Big\{(A_2y - B_2 + C_2)\int_{\zeta=0}^{(1-y)^{1/p}}(\zeta^p-1)(2-\zeta^p)^{1/p-1}\,d\zeta\\ &+ B_2\int_{\zeta=0}^{(1-y)^{1/p}}\zeta^p(\zeta^p-1)(2-\zeta^p)^{1/p-1}\,d\zeta\Big\}(1-y^2)^{1/p}\Big]\,dy\end{aligned} \tag{29}$$

where

$$A_1 = (a^2 - b^2)\,\sin\alpha\,\cos\alpha,\;\; B_1 = h\,(a^2\cos^2\alpha + b^2\sin^2\alpha),\;\; C_1 = -y_0\,A_1 - \zeta_0\,B_1 \tag{30a}$$

$$A_2 = a^2\,\sin^2\alpha + b^2\,\cos^2\alpha,\quad B_1 = h\,A_1,\quad C_2 = -y_0\,A_2 - \zeta_0\,B_2 \tag{30b}$$

Evaluation of the repeated integrals by numerical quadrature is considered in the next section.

6. NUMERICAL EXAMPLES

Two representative examples are considered in this section: one for $h = 1$ (square duct) and $h = 1/2$ (a rectangular duct with one-half height compared to the width). Melling and Whitelaw (1976) covers the case of a square duct, and Fig. 13 of their experiment is suggestive of an elliptic patch vortex with $y_0' = 0.40$, $z_0' = 0.25$ or, $y_0 = 0.40$ and $\zeta_0 = -0.75$. Equation (19) then gives $r = 0.65$ with $\alpha = \pi/8$. Equations (22) and (21) then approximately give $a = 0.43$ and $b = 0.20$, and Eqs. (26a) and (26b) yield for the elliptic patch, the velocity field

$$\bar{v} = \omega\,(0.45558\,y + 1.45550\,z + 0.90947) \tag{31a}$$

$$\bar{w} = -\omega\,(0.54442\,y + 0.45558\,z + 0.12388) \tag{31b}$$

with the equation of the ellipse [Eqs. (23a) and (23b)] in y-z coordinates as

$$y = 0.40 + 0.39727\,\cos\phi + 0.07684\,\sin\phi \tag{32a}$$

$$z = -0.75 + 0.18551\,\sin\phi - 0.16455\,\cos\phi,\quad (0 \le \phi \le 2\pi) \tag{32b}$$

The vector plot of Eqs. (31a) and (31b) together with that of the ellipse (32a) and (32b) is shown in Fig. 5. The velocity plot near the center of the duct appears comparatively larger than in the experiment of Melling and Whitelaw (1976). It is due to the suctional effect of the primary flow in the central core of the duct.

The computation of the wall resistance from Eq. (29) requires numerical integration with respect to y and ζ variables. This is accomplished by integrating the outer y integral by Simpson's rule by dividing the range $(0,\,1)$ in to 100 equal-sized panels, while evaluating the inner ζ integral by using the ADAPTIVE_SIMPSON subroutine given

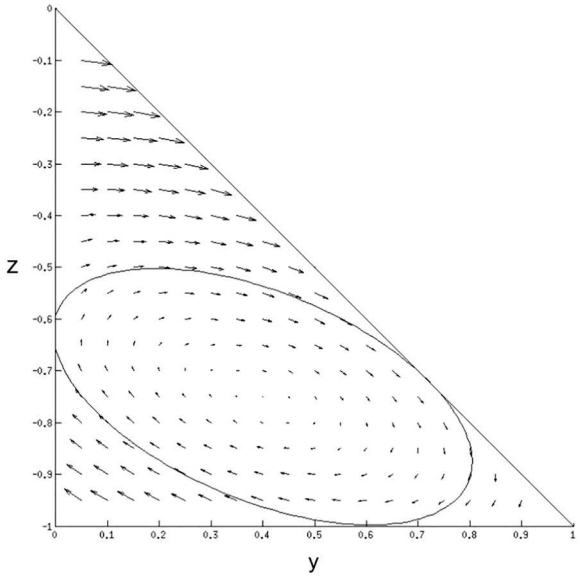

FIG. 5: Velocity plot in an octant for a square duct

in Bose (2009), which uses an adaptive selection of grid points for the Simpson's rule. The procedure yields, using Eq. (8),

$$2\,\tau_0 = 0.13690\,U_0\rho\omega = 0.16102\,U\,\rho\omega \tag{33}$$

The left-hand side of Eq. (33) represents the resistance to forward flow by the base of length 2, on a unit length of the duct. The other three walls of the duct exert identical resistance. Evidently, the resistance is increased by the secondary circulation of flow.

In the second example, a rectangular duct with $h = 1/2$, for which $\alpha = (1/2)\arctan(1/2) = 0.23183$ is considered. The center of the elliptic patch is taken to be at $y_0 = 0.3$, yielding $z_0' = (1 - y_0)\tan\alpha \approx 0.17$ and therefore $\zeta_0 = -0.66$. Accordingly, from Eq. (19), $r \approx 0.72$, and from Eqs. (21) and (22), $a \approx 0.31$ and $b \approx 0.12$. From Eqs. (26a) and (26b) the velocity field in the vertical patch thus becomes

$$\bar{v} = \omega\,(0.33068\,y + 1.66136\,z + 0.44904) \tag{34a}$$

$$\bar{w} = -\omega\,(0.33864\,y + 0.33068\,z + 0.00753) \tag{34b}$$

and the equation of the ellipse from Eqs. (23a) and (23b) in y-z coordinates is

$$y = 0.30 + 0.30171\,\cos\phi + 0.03525\,\sin\phi \tag{35a}$$

$$z = -0.33 + 0.14931\,\sin\phi - 0.07123\,\cos\phi, \quad (0 \le \phi \le 2\pi) \tag{35b}$$

The vector plot of the velocity field given by Eqs. (34a) and (34b) and that of the ellipse (35a) and (35b) is given in Fig. 6.

The computation of the wall resistance given by Eq. (29) is carried out as in the case of a square duct. In this case it is found that

$$2\,\tau_0 = 0.03192\,U_0\,\rho\omega = 0.03754\,U\,\rho\omega \tag{36}$$

Equation (36) gives the shear resistance by the base on a unit length of the duct. Evidently, for the same value of U, ρ, ω the secondary flow resistance is lower in this case compared to that of a square duct. From symmetry, the upper wall whose length is also 2 exerts identical resistance, but the two shorter vertical walls each of length $2h$ exert a different shear resistance τ_1 per unit length of the wall on a unit length of the duct. τ_1 can be simply determined

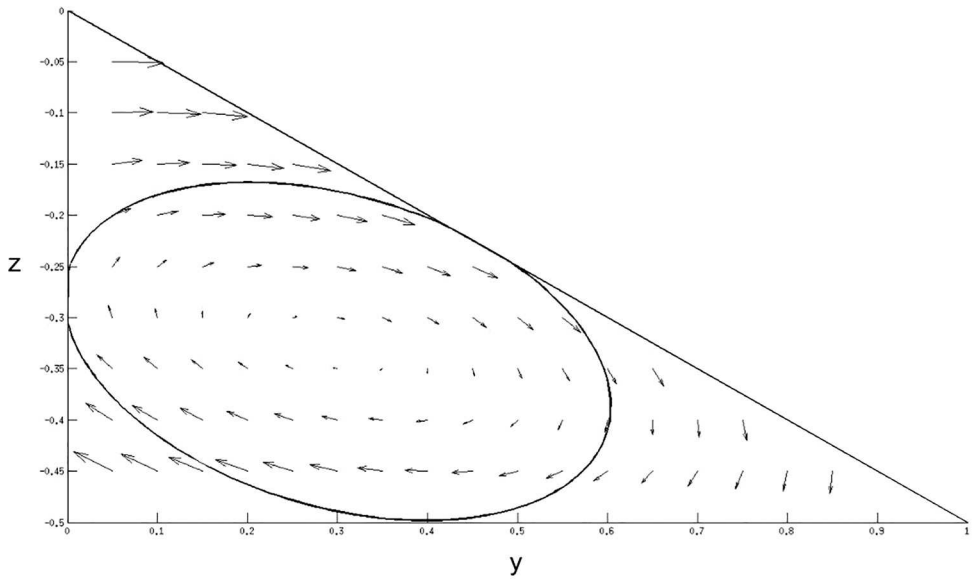

FIG. 6: Velocity plot in an octant for a rectangular duct $h = 1/2$

by consdering the vortical motion $-\omega$ in the upper triangle of the fourth quadrant. This yields, as in the case of Eq. (36),

$$2h\,\tau_1 = 0.03754\,U\,\rho\omega$$

or since $h = 1/2$,

$$\tau_1 = 0.03754\,U\,\rho\omega \tag{37}$$

Equation (36) gives the wall resistance to the secondary flow on a vertical side of the duct. An equal amount of resistance is exerted by the opposite side of the duct.

7. DISCUSSION AND CONCLUSIONS

Uniform steady turbulent incompressible fluid flow in rectangular ducts is accompanied by vortical, secondary flow in transverse sections of the duct. This secondary flow has been consistently detected in a number of experimental studies by different authors using hot-wire as well as laser Doppler anemometers (LDA). According to Prandtl (1952), kinematically the mean streamwise vorticity of the secondary flow is caused by the mean flow skewness, and kinetically by the inhomegeneity in anisotropy of the wall turbulence of the duct. The latter cause has been investigated by a number of authors.

This paper begins from the Reynolds averaged Navier–Stokes (RANS) equations. For mean uniform flows in the streamwise direction, the continuity equation kinematically governs the secondary motion in transverse sections, leading to a stream function which is analogous to the Prandtl's stress function that solves the torsion problem of an isotropic prismatic elastic beam. The symmetry of the duct with respect to the pair of bisectors of the side walls and the two diagonals, divides a cross section into eight equal parts, and it is sufficient to consider only one of the octants for study (Fig. 2). If it is assumed that the vorticity in an octant is nearly uniform as it is small, then the flow pattern in a square duct is like that in Fig. 3. This flow pattern is like that of Brundrett and Baines (1964). However, the more recent LDA measurements by Melling and Whitelaw (1976) indicates an oval-shaped vortical patch pushed toward a corner of the duct by the mean streamwise flow. Assuming elliptic form of a corner patch, Figs. 5 and 6 show the flow patterns for a square duct and a rectangular duct whose height is one-half of its base. The boundary condition in the first model, though exactly satisfied, the condition is only approximately satisfied in the vortical patch model. In the RANS momentum equations only the streamwise component is of significance. In this equation the streamwise mean velocity is approximately assumed to be given by the $1/p$th power law of the wall, where $p \approx 7$, such as in Schlichting (1979). The transverse velocities are modeled by the elliptic patch. Integration of the momentum equation over a cross section by numerical methods leads to an equation giving the total wall resistance in terms of the vorticity of the secondary flow and the primary mean flow velocity. Validation by well-controlled experimental data is required, as those of Melling and Whitelaw (1976) show some skewness. There is scope of applying the modeling method to study the same problem for incompletely filled ducts or open rectangular channels.

ACKNOWLEDGMENTS

The author is thankful to the S.N. Bose National Center for Basic Sciences, Kolkata for providing necessary facilities for undertaking this research, in particular to Dr. Amlan Dutta. Gratitude also goes to Professor Renu Bajaj, Department of Mathematics, Panjab University, Chandigarh for providing necessary literature on the topic of this research.

REFERENCES

Abramowitz, M. and Stegun, I.A., *Handbook of Mathematical Functions*, New York: Dover Publications, 1972.

Ahmed, S. and Brundrett, E., Turbulent flow in rectangular ducts. Mean flow properties in the developing region of a square duct, *Int. J. Heat Mass Transfer*, vol. **14**, pp. 365–375, 1971.

Bose, S.K., *Numeric Computing in Fortran*, New Delhi: Narosa Publications, 2009.

Brundrett, E. and Baines, W.D., The production and diffusion of vorticity in duct flow, *J. Fluid Mech.*, vol. **19**, pp. 375–394, 1964.

Gessner, F.B., The origin of secondary flow in turbulent flow along a corner, *J. Fluid Mech.*, vol. **58**, pp. 1–25, 1973.

Gessner, F.B. and Jones, J.B., On some aspects of fully-developed turbulent flow in rectangular channels, *J. Fluid Mech.*, vol. **23**, pp. 689–713, 1965.

Gradshteyn, I.S. and Ryzhik, I.M., *Table of Integrals, Series, and Products*, New York: Academic Press, 1980.

Hoagland, L.C., Fully developed turbulent flow in straight rectangular ducts, PhD thesis, Massachusetts Institute of Technology, USA, 1960.

Launder, B.E. and Ying, W.M., Secondary flows in ducts of square cross-section, *J. Fluid Mech.*, vol. **54**, pp. 289–295, 1972.

Leutheusser, H.J., Turbulent flow in rectangular ducts, *J. Hyd. Div., Proc. ASCE*, vol. **89**, pp. 1–19, 1963.

Melling, A. and Whitelaw, J.H., Turbulent flow in rectangular duct, *J. Fluid Mech.*, vol. **78**, pp. 289–315, 1976.

Nikuradze, J., *Untersuchungen über die Geschwindigkeitsverteilung in turbuleten Strömungen*, Berlin: VDI-Verlag, 1926.

Perkins, H.J., The formulation of streamwise vorticity in turbulent flow, *J. Fluid Mech.*, vol. **44**, pp. 721–740, 1970.

Prandtl, L., *Essentials of Fluid Dynamics*, London: Blackwell, 1952.

Schlichting, H., *Boundary-Layer Theory*, New York: McGraw-Hill, 1979.

Sokolnikoff, I.S., *Mathematical Theory of Elasticity*, New York: McGraw-Hill, 1956.